BioPAL *New ways to make measurements in the life sciences.*
BioPhysics Assay Laboratory, Inc. 80 Webster Street Worcester MA 01603 Phone (508) 770-1190 Fax (508) 770-1191 www.biopal.com

Application Note 3.

Title. Cell Labeling Method using **M**olday **ION Rhodamine B™** (**CL-50Q02-6A-50)**, a Fluorescent Cationic USPIO JRH/EVG

Keywords.
Molday **ION™**, MION, USPIO, SPIO, MRI, Prussian blue, rhodamine B, fluorescence, nanoparticle, iron oxide, colloid, cell labeling, BioPAL.

Summary.

Nanoparticles are increasingly used to label cells, to track them by imaging or to quantify them *in vivo*. However, normal cellular uptake mechanisms are inadequate to load cells with a tracking label. We have prepared a non-transfection-based fluorescent iron-oxide nanoparticle that is easily taken up by a variety of cells, reaching levels suitable for tracking. The following 10 cell types from four classes of cells have been labeled: *adherent cells*, NIH-3T3 (Murine Embryonic Fibroblasts), MCF-7 (Human Breast Adenocarcinoma), ATDC-5 (Murine Chondrocytic Cells); *primary cells*, HUVEC (Human Umbilical Vein Endothelial Cells), Primary Mouse Embryonic Fibroblasts-gamma irradiated; *stem cells*, hESC (Human Embryonic Stem Cells H1 p-36), C17.2 (Murine Neural Stem Cells), hMSC (Human Mesenchymal Stem Cells); *suspension cells*, KG-1 (Human Acute Myelogenous Leukemia Cells), NK-92 (Human Natural Killer Cells). Labeling is rapid (2-16 hours), uniform, and efficient (5-30% of the label is incorporated into cells). Labeled cells exhibit no signs of toxicity. Labeled cells can be stored frozen, thawed, and re-plated with levels of viability identical to untreated cells. The label appears to incorporate inside endosomes but is not found in the endoplasmic reticulum, golgi apparatus, nucleus, or any other cellular organelles. The nanoparticles are sterile and ready to use. Cell labeling is simple, chemically safe and typically requires no more than one hour of laboratory contact time.

Introduction.

Molday **ION** is a MION-like superparamagnetic iron oxide nanoparticle. These materials have been extraordinarily useful in a broad range of applications: immunoassays [1,2], detection and separation of cells, viruses, hormones, oligonucleotides, DNA and proteins [3-8], cell tagging, tracking, and imaging [9], targeted drug delivery [10]; gene delivery and therapy [11]; targeted hyperthermic treatment of cancer tissue [12], detoxification of biological fluids [13], and as a human MRI contrast agent for detection of liver tumor [14]. MRI provides valuable real-time cell tracking information in regenerative medicine [15-17]. Recent interest has focused on developing *ex vivo* cell labeling methods using MION and other ultrasmall superparamagnetic iron oxide nanoparticle contrast agents (USPIO) for analytic uses in development of cell therapy technology.

There have been numerous issues surrounding *ex vivo* cell labeling using nanoparticles [18]. Ideally, one wants a material that will be rapidly and completely taken up by the target cells in culture. Unfortunately, dextran coated nanoparticles such as MION are not readily transported into the cell by normal nonspecific cell uptake mechanisms. Typically, less than 1% of MION is internalized by cellular endocytosis [19-21]. This low level of incorporation of the MRI contrast agent MION stresses the already low sensitivity of MRI technology. Accordingly, researchers have conjugated a variety of agents to nanoparticles, including MION, to increase the percentage uptake of nanoparticles. These agents have not proven to have widespread applicability due to either the difficulty of preparing such conjugated nanoparticles or the difficulty of obtaining the targeting moieties [22]. Nevertheless, researchers have pursued a number of avenues to improve the ability of nanoparticles to label cells [23,24].

This application note presents a simple method for labeling cells using **CL-50Q02-6A** and **CL50Q02-6A-50**, both MION like iron oxide nanoparticles. These materials label cells with high efficiency thereby presenting a general solution to cell labeling with MRI contrast agents.

Materials and Methods.

CL-50Q02-6A-50, Molday **ION Rhodamine B** [2mg Fe/ml]	BioPAL
CL-50Q02-6A, Molday **ION** C6Amine [5mg Fe/ml]	BioPAL
CL-01-50 Prussian Blue Reagent Pack	BioPAL
CL-01-52 25% Glutaraldehyde	BioPAL
CL-01-53 40% Formalin	BioPAL
CL-01-51 PBS++	BioPAL

Note on nomenclature. CL-50Q02-6A-50 and **M**olday **ION Rhodamine B** are used interchangeably to describe the same nanoparticle.

Cell Labeling

(1) Serum free labeling of cells. Cells were grown to 70% confluence in 0.5ml DMEM with 10% bovine calf serum (BCS) and 1X AAS in a 24-well plate at 37°C and 5% CO_2. The medium was aspirated and replaced with 0.5ml 37°C serum free DMEM medium, supplemented with **CL-50Q02-6A-50** at a concentration of 25ug Fe /ml. The cells were incubated 18 hours. The solution was aspirated after incubation. The cells were washed with Phosphate Buffered Saline supplemented with calcium and magnesium (PBS++) and covered with complete medium. The cells were visualized while living or fixed (2% formalin 2.5% glutaraldehyde) using an inverted fluorescent microscope (Nikon TE-2000-S).

(2) In an alternative procedure cells were labeled in medium supplemented with serum. Cells were plated in a 24-well plate ($1x10^5$ cells/well) in 0.5 ml DMEM containing 10% BCS (GIBCO) and incubated (humidified) at 37°C, 5% CO_2. After allowing the cells to adhere overnight, **CL-50Q02-6A-50** was added to serum supplemented medium and incubated for 16 hours. The medium was aspirated after incubation. The cells were washed with Phosphate Buffered Saline supplemented with 0.1g/L calcium and 0.1g/L magnesium (PBS++) and covered with complete medium. The cells were visualized while living or fixed (2% formalin 2.5% glutaraldehyde) using an inverted fluorescent microscope (Nikon TE-2000-S).

Cell Fixation

The cells were washed at 37°C with PBS++ and fixed with a 2% formalin/2.5% glutaraldehyde solution in PBS++ for 10 minutes. The cells were washed again with PBS++ and stained using the Prussian Blue Reagent set (**CL-01-50)**. Detailed procedures for cell fixation and Prussian blue staining can be found on BioPAL's website (Application Notes 6 and 7, respectively).

Instrumental

Sizing. Colloids (**CL-50Q02-6A-50, CL-50Q02-6A, and CL-30Q02-2)** were sized by photon correlation spectroscopy using a 90 *Plus* particle size analyzer (Brookhaven Instruments Corp.). Samples were diluted to 1mg Fe/mL in saline, passed through a 0.1μm filter, and sonicated for one minute in a water-bath sonicator. A count rate between 50,000 and 500,000 counts per second was obtained. Data were collected for 4 cycles of 15 min and the cumulative results combined. Particle size was calculated by assuming refractive indexes of 1 and 0 for the real and imaginary components, respectively. Typical reproducibility for intra- and interassay variability yielded coefficients of variation of less than 6% and 9%, respectively. Nanoparticle sizes were calculated using an intensity-weighted log normal distribution.

Zeta Potential. Zeta potential measurements for representative colloids were determined using a 90 *Plus* particle size analyzer (Brookhaven Instruments Corp.) with zeta potential modification. Samples were diluted to a concentration of 1mg Fe/mL (total metals) in 1mM KCl, passed through a 0.1μm filter, and sonicated for one minute in a water-bath sonicator. Samples were run using the following instrument parameters: Sample count rate, ~700 kcps; sampling time, 1 minute; conductance, ~400μs; current, ~1.05mA, electric field ~7.5V/cm. Data is reported as the mean zeta potential (mV) of ten measurements.

Microscopy

Light microscopy (bright field, phase contrast, fluorescence) was performed using a Nikon TE-2000-S instrument with a 20X or 40X Plan Fluor objective. A "dsRED" filter set was used for the rhodamine channel.

Images were captured using a Diagnostics Instruments 18.2 Color Mosaic CCD camera. TEM images were obtained at the University of Massachusetts Medical School (Worcester) under the direction of Dr. Gregory Hendricks. Images were acquired on a Philips CM10 Electron Microscope at 4600X and 36000X magnification. Confocal microscopy was performed at the University of Massachusetts Medical School with the assistance of Dr. Furcinitti. Instrumentation included a Nikon TE-2000E2 microscope fitted with a Yokogawa CSU10 Spinning Disk Confocal Scan Head, a solid state laser illumination source (561nm), and a 100X Plan Apo Oil objective. Images were captured using a Photometrics Coolsnap HQ2 camera. The images were acquired at 200nm slices in the z-axis.

Results and Discussion.

Synthesis, chemical and physical properties. **M**olday **ION Rhodamine B (CL-50Q02-6A-50)** is a homogeneous, fluorescent iron oxide-based superparamagnetic (USPIO) contrast reagent designed to label cells efficiently and simply. **CL-50Q02-6A-50** can be visualized by both MRI and fluorescence. It is prepared from **CL-50Q02-6A** by reaction with rhodamine B isothiocyanate. Rhodamine B is a fluorescent dye with an excitation and emission wavelength of 555 and 565-620nm, respectively. The fluorescent spectrum of **CL-50Q02-6A-50** is nearly identical to that of rhodamine B (Figure 1). **CL-50Q02-6A-50** has an effective diameter of 35nm and a zeta potential of 31mV (Table 1) similar to its parent **CL-50Q02-6A**. The effective diameter and zeta potential of **CL-30Q02-2,** an unmodified USPIO, is included for comparison. The R1 and R2 values of **CL-50Q02-6A-50, CL-50Q02-6A, and CL-30Q02-2** are identical.

Figure 1. Fluorescent spectra of and rhodamine B. The blue and red lines represent spectra generated with **CL-50Q02-6A-50** and rhodamine B, respectively. The samples were dissolved in water at pH 7.4. **CL-50Q02-6A-50** and rhodamine B exhibit emission maxima at 579 and 581, respectively. The baseline is the spectrum of **CL-50Q02-6A** which contains no rhodamine B and is the precursor to **CL-50Q02-6A-50.**

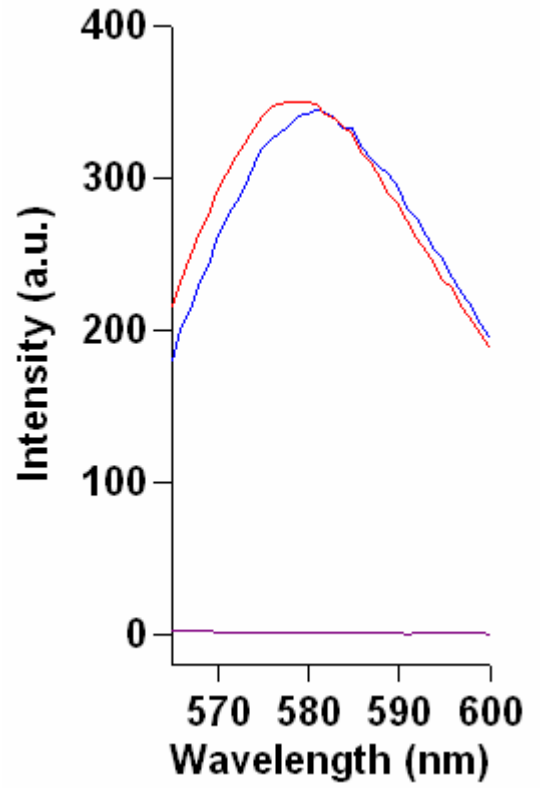

Table 1. Comparison of size, zeta potential, and relaxivity for three USPIO nanocolloids. Size and zeta potential were performed as described in Methods.

Compound	Effective diameter (nm)	Zeta potential (mV)	R1 $s^{-1}mM^{-1}$	R2 $s^{-1}mM^{-1}$
CL-30Q02-2	28	-5	15.4	33.9
CL-50Q02-6A	35	+48	16.5	34.8
CL-50Q02-6A-50	35	+31	16.3	34.2

Generality of Cell Labeling. Thus far, ten cell lines have been challenged with **CL-50Q02-6A-50** (**M**olday **ION Rhodamine B**) (Figure 2 and Table 2). All ten cell lines [see Table 2 for the description of cell types] efficiently internalized this nanoparticle. Figure 2 shows seven cell lines labeled with **CL-50Q02-6A-50** including adherent, suspension, primary and stem cell lines.

Dose response of cell labeling. NIH-3T3 cells exhibit a direct relationship between the concentration of **CL-50Q02-6A-50** and amount of nanoparticle uptake. This relationship is illustrated in Figure 3, a montage of cells labeled with three decreasing (left to right) concentrations of **CL-50Q02-6A-50**. The top row represents the rhodamine fluorescence channel and the bottom row is the paired bright field image. Careful inspection shows excellent overlap of the fluorescent and bright field images. Fluorescence is seen in vesicles contained within the cell body with complete exclusion from the nucleus. The cells showed no signs of growth inhibition or toxicity from exposure to the reagent.

*Cellular location of **CL-50Q02-6A-50**.* Examination of NIH-3T3 cells labeled with **M**olday **ION Rhodamine B** using light microscopy with Prussian blue iron staining and fluorescence (Figure 4), confocal multisliced imaging (fluorescence and DIC) (Figure 5), and transmission electron microscopy (Figure 6) consistently showed that **M**olday **ION Rhodamine B** was found only in endosomes. It did not localize to the nucleus, mitochondria, endoplasmic reticulum, Golgi apparatus, or any other cellular organelle. Close examination of multiple TEM fields showed no traces of electron dense material corresponding to **CL-50Q02-6A-50** on the surface of cells post labeling.

*Viability of NIH-3T3 cells labeled with **M**olday **ION Rhodamine B** following one freeze thaw cycle.* NIH-3T3 cells labeled with **CL-50Q02-6A-50** can be stored cryogenically, thawed and grown without noticeable changes compared to similarly treated unlabeled control cells. NIH-3T3 cells were treated with **CL-50Q02-6A-50** (25ug/ml) for 24 hours per the usual loading protocol. The cells were collected via typical passaging procedure. The medium was aspirated and discarded, the confluent layer of cells was rinsed with 37°C PBS, aspirated, and then trypsin/EDTA solution (brought to 37°C) was added. The cells were collected with a serological pipette and placed into a 15-ml centrifuge tube with high serum medium (20% serum/80% DMEM) to inactivate the trypsin. The cells were collected by centrifugation and resuspended in 50% serum, 45% DMEM, and 5% DMSO. The cell suspension was transferred into 2-ml cryovials, cooled at 1°C/min to -80°C for 24 hours, and placed into a liquid nitrogen dewar for extended storage. Thirty days after storage in liquid nitrogen, labeled and unlabeled control cells were thawed in a 37°C water bath. One ml of each thawed cell suspension was added to 9-ml of 37°C complete medium, mixed, and centrifuged to collect the cells. The pellet was re-suspended in fresh 37°C complete medium and seeded into appropriate vessels. The trypan blue dye exclusion test was performed to test cell viability. Ninety five percent of control and labeled cells were viable. Micrographs of NIH-3T3 cells labeled with **CL-50Q02-6A-50** were compared prior to freezing (Figure 7A) and after cryostorage and replating (Figure 7B and C). The pre- and post-frozen cells labeled with **CL-50Q02-6A-50** showed identical images with respect to general appearance and labeled vesicle distribution within the cells. Normal cell growth without observable aberrations following replating supported our conclusion that crystorage did not adversely effect **CL-50Q02-6A-50** labeled cells. Furthermore, the daughter cells in these post-cryogenic cultures visually contained half as much **CL-50Q02-6A-50 (**as indicated by fluorescence) compared to their progenitors. Fluorescence label was visible through four generations before becoming too dim to observe.

*Retention of **CL-50Q02-6A-50** within NIH-3T3 cells.* Confluent NIH-3T3 cells labeled with **CL-50Q02-6A-50** retained **CL-50Q02-6A-50** with minimal change in nanoparticle distribution and cell appearance. NIH-3T3 cells were plated into a T-25 flask and grown to confluence. The cells were then treated with 25ug/ml **CL-50Q02-6A-50** in 10% serum DMEM medium for 24 hours. The solution was washed out, replaced with reduced serum containing DMEM (5% serum), and maintained with the reduced serum medium to reduce cell growth for 4 weeks. The cellular retention of **CL-50Q02-6A-50** was monitored by fluorescent microscopy. The labeled cells retained fluorescent material inside vesicles for the duration of the study. Although cell growth was slowed, it was not completely stopped. Furthermore, as would be expected with unlabeled cells, a small fraction of the labeled cells died and were replaced by newly divided cells. When the cells divided, the amount of **CL-50Q02-6A-50** in the daughter cells was half of that from the original cell. Even after four weeks a large number

of cells retained **CL-50Q02-6A-50**. Throughout the 4 weeks of the experiment the cell free medium-supernatant was monitored for fluorescence of **CL-50Q02-6A-50**. No fluorescence was detected in the supernatant suggesting that most of **CL-50Q02-6A-50** was retained within the cells.

Conclusion.

Molday **ION Rhodamine B** labels cells efficiently, is retained within the cell for extended time periods, and is well tolerated. The labeling procedure is quick, safe, easy, and does not require the use of transfection reagents. Cell labeling requires adding **M**olday **ION Rhodamine B** directly to the cell medium which is then applied to cells. **M**olday **ION Rhodamine B** offers: (i) the ability to label cells *in vitro* and then track the cells *in vivo* using MRI, fluorescence, or staining of biopsied samples; (ii) opportunity to conjugate ligands for specific targeting and imaging applications *in vitro* or *in vivo*; (iii) multiple platforms for dual drug delivery and imaging system; (iv) magnetic manipulation for targeting *in vivo*, isolation from tissues and post labeling purification; (v) magnetic/RF hyperthermic treatment. Research applications include cardiovascular and vascular imaging, cell labeling and tracking, drug delivery, and magnetic cell sorting.

Figure 2. The 7 paired photomicrographs are a sample of cell types labeled with **M**olday **ION Rhodamine B**. The images are paired Phase1 contrast (left side of split panels) and fluorescence (right side of split panels). All photomicrographs were obtained at 200X magnification. The bar represents 20μm.

NIH-3T3 (Murine Embryonic Fibroblasts)

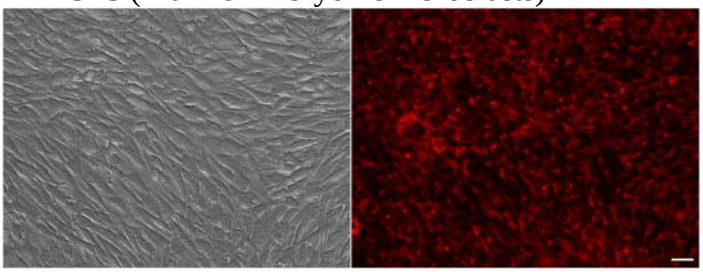

MCF-7 (Human Breast Adenocarcinoma)

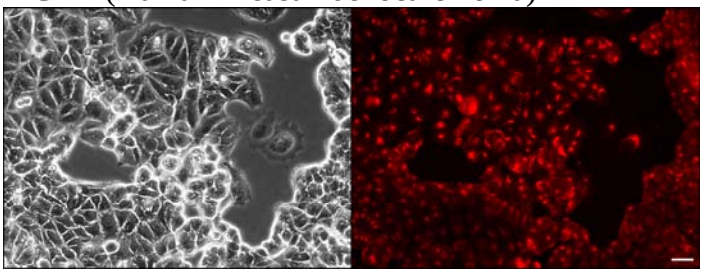

ATDC-5 (Murine chondrocytic cells

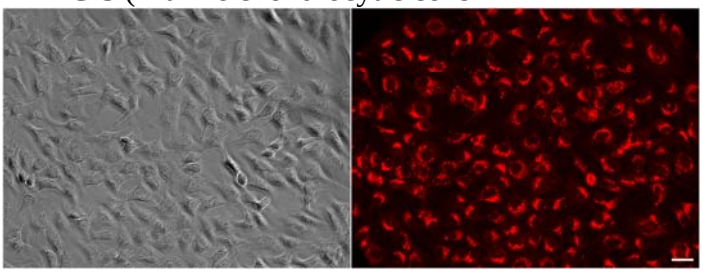

HUVEC (Human Umbilical Vein Endothelial Cells)

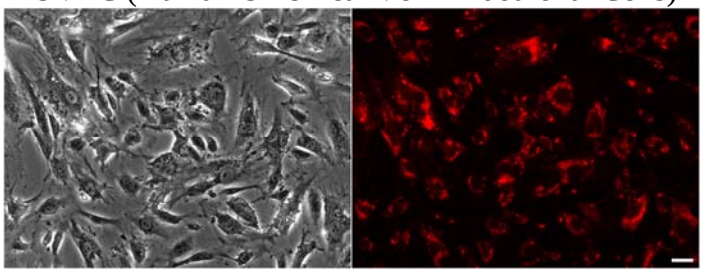

C17.2 (Murine Neural Stem Cells)

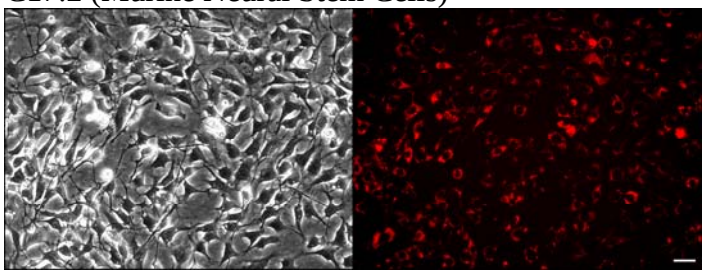

hESC (Human Embryonic Stem Cells H1 p-36)

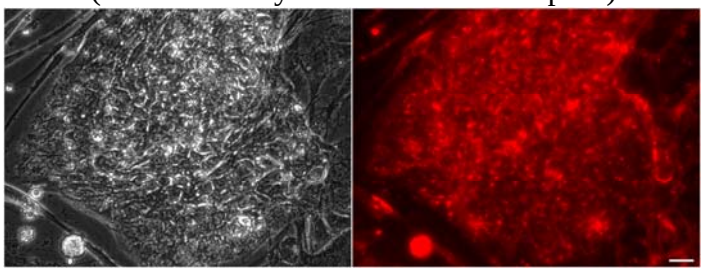

KG-1 (Human Acute Myelogenous Leukemia cells)

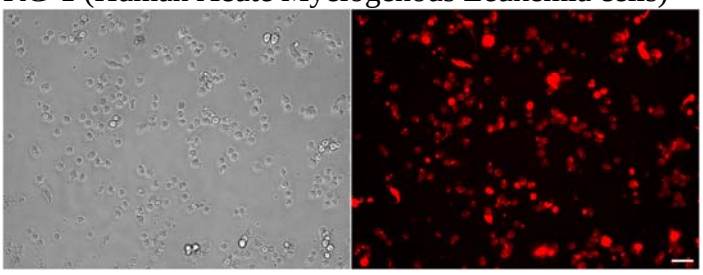

Table 2. List of cells tested with **CL-50Q02-6A-50**. All cells showed a healthy appetite for the nanoparticle.

Adherent Cells	NIH-3T3 (Murine Embryonic Fibroblasts)	MCF-7 (Human Breast Adenocarcinoma)	ATDC-5 (Murine chondrocytic cells
Primary Cells	HUVEC (Human Umbilical Vein Endothelial Cells)	Primary Mouse Embryonic Fibroblasts	
Stem Cells	C17.2 (Murine Neural Stem Cells)	hESC (Human Embryonic Stem Cells H1 p-36)	hMSC (Human Mesenchymal Stem Cells)
Suspension Cells	KG-1 (Human Acute Myelogenous Leukemia cells)	NK-92 (Natrual Killer cells)	

Figure 3. Relationship between **CL-50Q-02-6A-50** concentration and cell uptake in NIH-3T3 cells. Cells were plated in a 24-well plate ($1x10^5$ cells/well) in 0.5 ml DMEM containing 10% bovine serum (GIBCO) and incubated (humidified) at 37°C, 5% CO_2. After allowing the cells to adhere overnight, fluorescently conjugated nanoparticles (**CL-50Q-02-6A-50**) were added to the medium and incubated for 16 hours. Cells in column A, B, and C contained 50, 12.5, and 0.5 µg Fe/ml, respectively. The cells were fixed with a 2% formalin, 2.5% glutaraldehyde solution and stained with Prussian Blue. The bar in the bottom right corner represents 10µm. 400x400 sections were cropped out of the full size image and placed into a montage using the program ImageJ, version 1.41O.

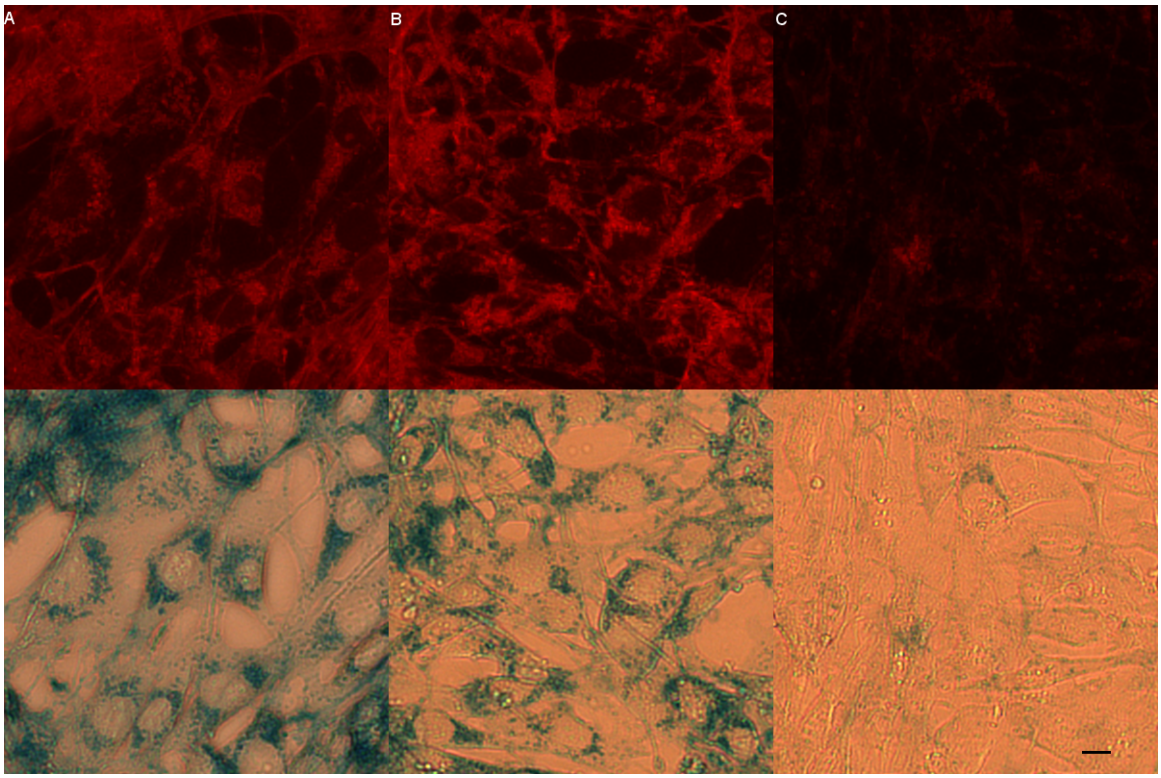

Figure 4. Co-localization of iron staining and fluorescence in NIH-3T3 cells labeled with **M**olday **ION Rhodamine B**. The cells were fixed and stained for iron using Prussian Blue Reagent Pack. Panel A iron stain (Phase 2 contrast) and Panel B (fluorescence, rhodamine B channel) shows coincidence for the two visualization methods. Images were obtained at 400X magnification. The bar represents 20µm.

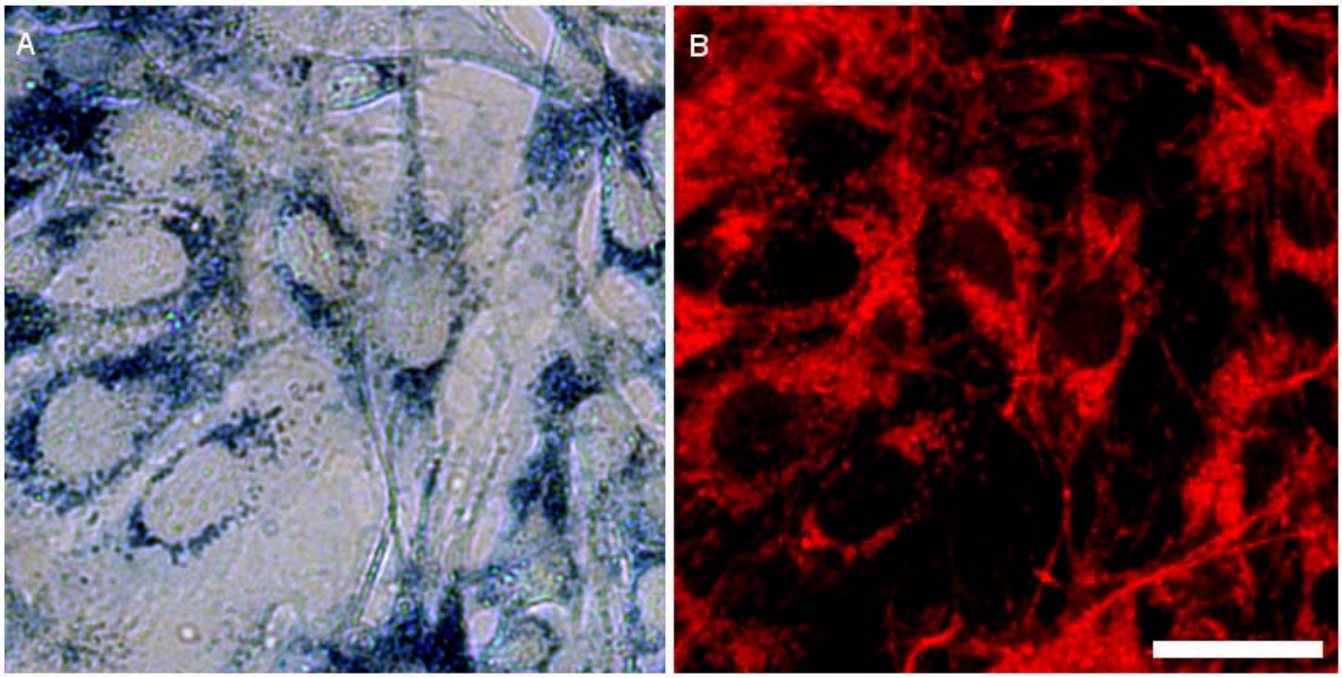

Figure 5. Confocal microscopy images of NIH-3T3 cells labeled with **M**olday **ION Rhodamine B**. Cells were incubated with **M**olday **ION Rhodamine B** for 18 hours and then fixed with 2% formalin 2.5% glutaraldehyde. **M**olday **ION Rhodamine B** localizes within the cell body in small vesicles and is not found on the cell surface. Left Panel. 1000X magnification confocal images, each image represents a slice obtained every 2.2 μm. The four images (left to right) start at the bottom of the cell and end at the top of the cell. Top row is DIC, middle row is composite DIC and fluorescence, bottom row is fluorescence. The bar represents 10μm. Right Panel. Confocal composite image of DIC and rhodamine channels shows **M**olday **ION Rhodamine B** inside vesicles. The bar represents 10μm.

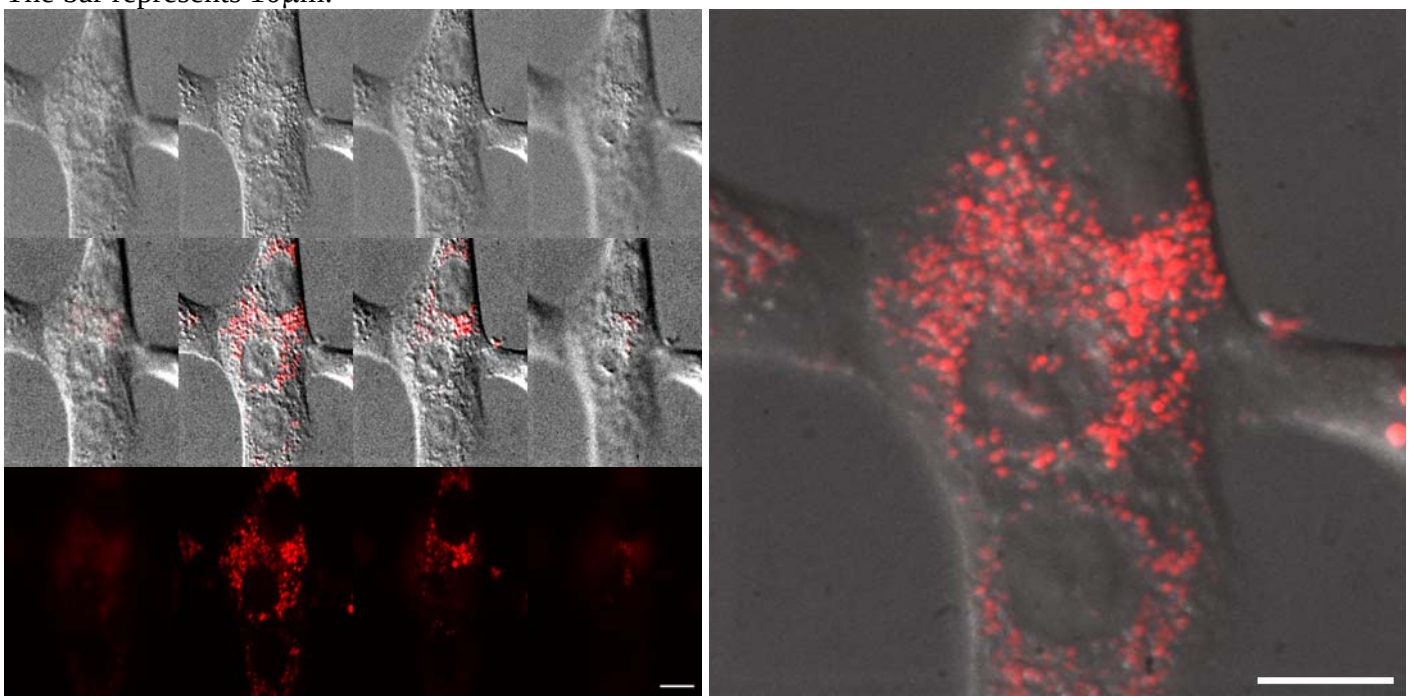

Figure 6. TEM images of NIH-3T3 cells labeled with **M**olday **ION Rhodamine B**. The left TEM image represents a cell labeled with **M**olday **ION Rhodamine B** (25ugFe/ml) at a magnification of 4600X (bar=2μm). Dark vesicles can be seen inside the cytoplasm of the cell; each vesicle is packed with electron dense **M**olday **ION Rhodamine B**. The white square outlines the area magnified [36000X (bar=200nm)] and presented in the right image showing two vesicles loaded with **M**olday **ION Rhodamine B**. The small dark spheres are the iron oxide cores of the nanoparticles.

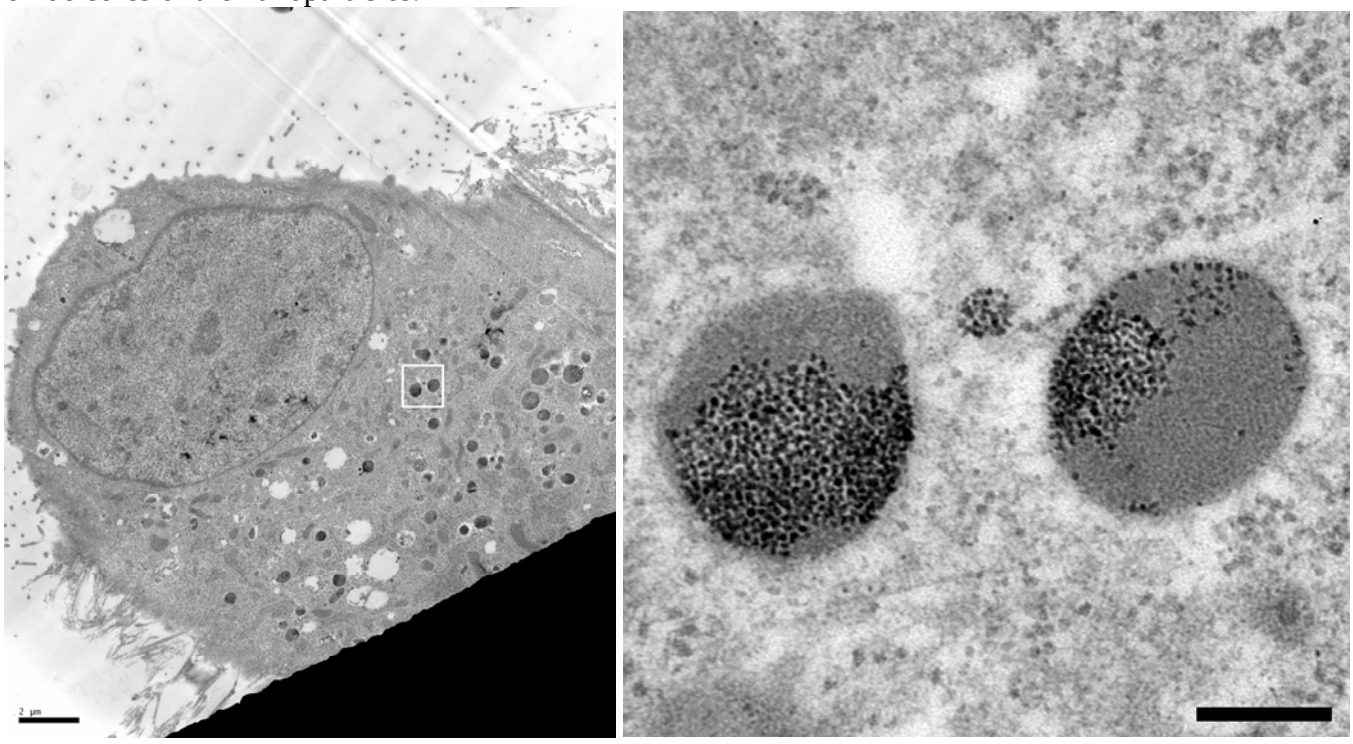

Figure 7. Comparison of NIH-3T3 cells labeled with **CL-50Q02-6A-50** pre- and post-cryogenic storage. Panel A shows a fluorescent image (rhodamine B channel) of NIH-3T3 cells labeled with **M**olday **ION Rhodamine B** before cryogenic storage. Panels B and C show paired images of the same cells after cryogenic storage and revival. Panel B is a Phase 2 contrast image and Panel C is a fluorescent image (rhodamine B channel). All images were obtained at 400X magnification. The bar represents 10μm.

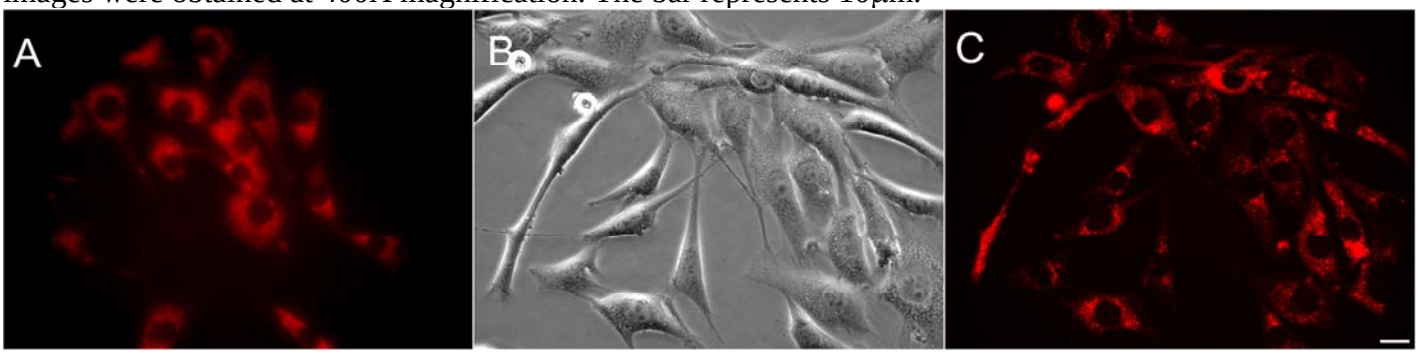

References

1. Druet, E., Mahieu, P., Foidart, J. M., and Druet, P. [1982] Magnetic solid-phase enzyme immunoassay for the detection of anti-glomerular basement membrane antibodies. *J Immunol Methods 48*, 149-157.
2. Guesdon, J. L., Thiery, R., and Avrameas, S. [1978] Magnetic enzyme immunoassay for measuring human IgE. *J Allergy Clin Immunol 61*, 23-27.
3. Gu, H., Ho, P. L., Tsang, K. W., Yu, C. W., and Xu, B. [2003] Using biofunctional magnetic nanoparticles to capture gram-negative bacteria at an ultra-low concentration. *Chem Commun [Camb]*, 1966-1967.
4. Pazzagli, M., Kohen, F., Sufi, S., Masironi, B., and Cekan, S. Z. [1988] Immunometric assay for lutropin [hLH] based on the use of universal reagents for enzymatic labelling and magnetic separation and monitored by enhanced chemiluminescence. *J Immunol Methods 114*, 61-68.
5. Vonk, G. P., and Schram, J. L. [1991] Dual-enzyme cascade-magnetic separation immunoassay for respiratory syncytial virus. *J Immunol Methods 137*, 133-139.
6. Josephson, L., Perez, J., and Weissleder, R. [2001] Magnetic nanosensors for the detection of oligonucleotide sequences. *Angew. Chem., Int. Ed.. 40*, 3204-3206.
7. Patolsky, F., Weizmann, Y., Katz, E., and Willner, I. [2003] Magnetically amplified DNA assays [MADA]: Sensing of viral DNA and single-base mismatches by using nucleic acid modified magnetic particles. *Angew. Chem,. Int. Ed. 42*, 2373-2376.
8. Nam, J. M., Thaxton, C. S., and Mirkin, C. A. [2003] Nanoparticle-based bio-bar codes for the ultrasensitive detection of proteins. *Science 301*, 1884-1886.
9. Lewin, M., Carlesso, N., Tung, C. H., Tang, X. W., Cory, D., Scadden, D. T., and Weissleder, R. [2000] Tat peptide-derivatized magnetic nanoparticles allow in vivo tracking and recovery of progenitor cells. *Nat Biotechnol 18*, 410-414.
10. Hafeli, U. O. [2004] Magnetically modulated therapeutic systems. *Int J Pharm 277*, 19-24.
11. Xiang, J. J., Tang, J. Q., Zhu, S. G., Nie, X. M., Lu, H. B., Shen, S. R., Li, X. L., Tang, K., Zhou, M., and Li, G. Y. [2003] IONP-PLL: a novel non-viral vector for efficient gene delivery. *J Gene Med 5*, 803-817.
12. Jordan, A., Scholz, R., Maier-Hauff, K., Johannsen, M., Wust, P., Nadobny, J., Schirra, H., Schmidt, H., Deger, S., Loening, S., Lanksch, W., and Felix, R. [2001] Presentation of a new magnetic field therapy system for the treatment of human solid tumors with magnetic fluid hyperthermia. *J. Magn. Magn. Mater. 225*, 118-126.
13. Gupta, A. K., and Gupta, M. [2005] Synthesis and surface engineering of iron oxide nanoparticles for biomedical applications. *Biomaterials 26*, 3995-4021.

14. Marchal, G., Van Hecke, P., Demaerel, P., Decrop, E., Kennis, C., Baert, A. L., and van der Schueren, E. [1989] Detection of liver metastases with superparamagnetic iron oxide in 15 patients: results of MR imaging at 1.5 T. *AJR Am J Roentgenol 152*, 771-775.
15. Sakai, D., Mochida, J., Iwashina, T., Hiyama, A., Omi, H., Imai, M., Nakai, T., Ando, K., and Hotta, T. [2006] Regenerative effects of transplanting mesenchymal stem cells embedded in atelocollagen to the degenerated intervertebral disc. *Biomaterials 27*, 335-345.
16. Tallheden, T., Nannmark, U., Lorentzon, M., Rakotonirainy, O., Soussi, B., Waagstein, F., Jeppsson, A., Sjogren-Jansson, E., Lindahl, A., and Omerovic, E. [2006] In vivo MR imaging of magnetically labeled human embryonic stem cells. *Life Sci 79*, 999-1006.
17. Ye, Y., and Bogaert, J. [2008] Cell therapy in myocardial infarction: emphasis on the role of MRI. *Eur Radiol 18*, 548-569.
18. Stella, B., Arpicco, S., Peracchia, M. T., Desmaele, D., Hoebeke, J., Renoir, M., D'Angelo, J., Cattel, L., and Couvreur, P. [2000] Design of folic acid-conjugated nanoparticles for drug targeting. *J Pharm Sci 89*, 1452-1464.
19. Zimmer, C., Wright, S. C., Jr., Engelhardt, R. T., Johnson, G. A., Kramm, C., Breakefield, X. O., and Weissleder, R. [1997] Tumor cell endocytosis imaging facilitates delineation of the glioma-brain interface. *Exp Neurol 143*, 61-69.
20. Moore, A., Weissleder, R., and Bogdanov, A., Jr. [1997] Uptake of dextran-coated monocrystalline iron oxides in tumor cells and macrophages. *J Magn Reson Imaging 7*, 1140-1145.
21. Moore, A., Josephson, L., Bhorade, R. M., Basilion, J. P., and Weissleder, R. [2001] Human transferrin receptor gene as a marker gene for MR imaging. *Radiology 221*, 244-250.
22. Babic, M., Horak, D., Trchova, M., Jendelova, P., Glogarova, K., Lesny, P., Herynek, V., Hajek, M., and Sykova, E. [2008] Poly[L-lysine]-modified iron oxide nanoparticles for stem cell labeling. *Bioconjug Chem 19*, 740-750.
23. Shinkai, M. [2002] Functional magnetic particles for medical application. *J Biosci Bioeng 94*, 606-613.
24. Zhang, Y., and Zhang, J. [2005] Surface modification of monodisperse magnetite nanoparticles for improved intracellular uptake to breast cancer cells. *J Colloid Interface Sci 283*, 352-357.